

Green Synthesis of ZnO Nanoparticles Using Sallanum Santhocarbom to Study Its Solarphotocatalytic Activity

Karthiga Rajendaran¹, Sudha Annamalai¹

¹Theni Kammavar Sangam College of Arts and Science, Kammavar Nagar, Koduvilarpatti, Theni – 625534, India

E-mail: skarthika1121[at]gmail.com, sudhaguru2551994[at]gmail.com

Abstract: ZnO nanoparticles were prepared through a facile one part green synthesis method with assistance of sollanam santhocarbom plant. The as synthesized ZnO was subjected to UV-visible diffuse reflectance spectroscopy (UV-vis-DRS), fourier transformed infrared spectroscopy (FT-IR), X-Ray diffraction (XRD), Scanning Electron Microscopy (SEM) and energy dispersive X-ray Spectroscopy (EDS). The solar photocatalytic activity of nanoparticles was evaluated by degradation of Fuchsine (FU) in aqueous solution. The plant extract modified ZnO exhibited the highest photocatalytic activity under sunlight illumination with a dye concentration of 10µm/L and it follows pseudo first order kinetic.

Keywords: ZnO, Green synthesis, solar-photocatalysis, Fuchsine

1. Introduction

At the present time, the common industry processes are using dyes by textile industry to color their products. Since this industry also uses substantial amount of water in their processes to form highly colour effluent of this industry which generally has hazardous effect in our ecosystem due to the presence of these organic chemicals. So it was necessary to find a new way to remove colored dyes before discharging them into the environment [1, 2]. Heterogeneous photocatalytic degradation of refractory organic pollutants from water by semiconductors has attracted extensive attention in the past several decades [3–5]. Previous studies have proved that the wide-bandgap semiconductor photocatalyst such as TiO₂ and ZnO can degrade various organic pollutants under UV irradiation, which offers great potentials for the complete elimination of toxic chemicals [6,7]. It has been reported that ZnO had higher photocatalytic efficiency compared with TiO₂ in the degradation of several organic contaminants in both acidic and basic medium, which has stimulated many researchers to further explore the properties of ZnO in many photocatalytic reactions [8–10].

ZnO nanoparticles can be synthesized by various approaches including sol-gel processing [11], homogeneous precipitation [12], mechanical milling [13], organometallic synthesis [14], microwave method [15], spray pyrolysis [16], thermal evaporation [17] and mechanochemical synthesis [18]. However, chemicals used for nanoparticles synthesis and stabilization are toxic and lead to non-ecofriendly by products. Plant extract or plant biomass could be an alternative to chemical and physical method for the generation of metal oxide nanoparticles in an eco-friendly manner. Solanum xanthocarpum leaves have been reported to possess anti-implantation and anti spermatogenic activities [19, 20] and it can also been shown a protective effect against the tumour promotion stage of cancer development. The leaves and flowers are observed to be promoters of hair growth and aid in healing of ulcer [21]. Solanum

xanthocarpum leaves has antioxidant as their phytochemical which can act as reducing as well as capping agent. The phytochemical analysis of the flower extract of Solanum xanthocarpum leaves contains Tannins, saponins, alkaloids, steroids, flavonoids in the aqueous extract.

Therefore, developments of nanoparticles with high photocatalytic properties are of considerable interest. In the present study, direct precipitation method is used to synthesize ZnO nanoparticles using plant extract as a surface modifier has been studied. The solar photocatalytic activity for Fuchsine (FU) was studied using these synthesized nanoparticles under sun light irradiation. The study shows that SZO is a potential candidate as catalyst for solar photodegradation of FU in water with usage of very small amount of nanoparticles.

2. Materials and Methods

2.1 Materials

Solanum xanthocarpum plants were collected from in and around Theni district. All the chemicals used in this experiment were of analytical grade. Double distilled water was used throughout the experiments.

2.1.1. Experiment

(a) Preparation of plant extract

Thoroughly washed solanum xanthocarpum leaves 20 g were cut and boiled with 100 ml of double distilled water for 1h in hot plate at temperature 80 °C. Finally the plant extract was filtered through filter paper (what man no: 1) and stored in the refrigerator at 4 °C for further experiment [22].

(b) Preparation of plant extract modified ZnO

5g of ZnO was dissolved in 100ml of double distilled water. 1N NaOH added to the above solution with constant stirring

to adjust the pH of the solution to the above solution. 5ml of plant extract was added and stirring is continued for 5 h. The nanoparticle was and dried at room temperature and calcinated for 1h in a muffle furnace at 500 °C [23]. The same procedure is followed without plant extract for the preparation of ZnO. The schematic digram of prepared nanoparticle are shown in Figure 1.

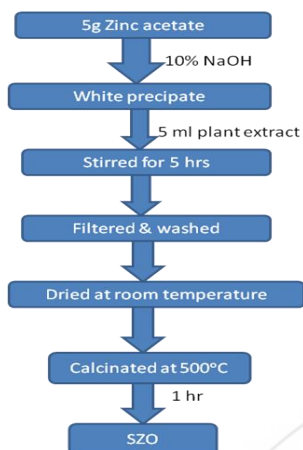


Figure 1: Schematic diagram of synthesis of SZO

1.2.1. Evaluation of Solar photocatalytic activity

For the photocatalytic evaluation, the aqueous solution of FU was used as the target pollutants. The degradation tests of FU aqueous solutions were carried out outdoors at noon on sunny days under solar light irradiation at room temperature (~35 °C) in September, Tamilnadu. For each test, 0.10 g of the as-prepared photocatalysts was dispersed in 100 ml of FU solutions with a concentration of 10µM in round bottom flask. The solution was then exposed to the sunlight directly and with regular time intervals of 30 min, the suspensions were centrifuged to remove the photocatalysts completely at 5000 rpm for 5 min. Aliquots of the residual transparent FU solutions were transferred to a cuvette for UV–visible spectroscopy for the absorption spectra. The photocatalytic efficiencies of different photocatalysts over FU are defined by the relative ratios of C/C₀, where C is the concentration of FU aqueous solution after sunlight irradiation at predefined time (t), and C₀ is their concentration at the equilibrium adsorption state. C and C₀ were determined by the relative absorbance (A/A₀) at 423 nm, where A is the absorbance of FU after sunlight irradiation at predefined time (t), and A₀ is the absorbance at equilibrium [24, 25]. The for the solarphotodegradation and the experimental setup was shown in Figure 2 and 3.

$$\text{Photodegradation percentage of Fu} = \frac{C_0 - C}{C_0} \times 100 \text{ ----- (1)}$$

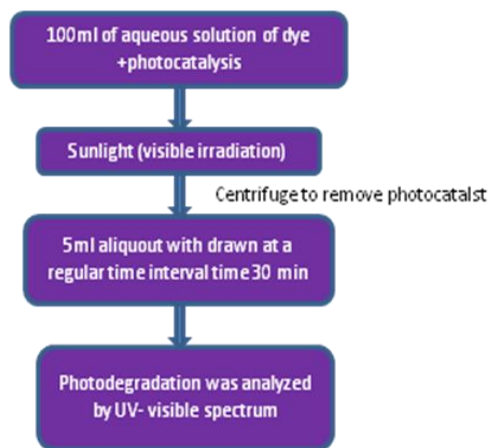


Figure 2: The schematic diagram for the Solar photodegradation of FU dye



Figure 3: Photograph of Solar Photoreactor setup

3. Result and Discussion

3.1 UV–Vis spectral studies

Figure 4 (a) shows the Uv –visible spectra of ZnO (SZO) and plant extract modified ZnO (SZO). The absorption SZO is red shifted when compared to ZO. This attribute due to the addition of plant extract with ZnO. The optical band gap E_g of the nanoparticles is determined by extrapolation of linear portion of α² versus hv plots using the plots using the following equation [26].

$$\alpha = \frac{C(h\nu - E_g^{\text{bulk}})^2}{h\nu} \text{ ----- (2)}$$

where α is the absorption co-efficient, hν is the photon energy. E_g optical band gap energy and c is the constant depending on the electron – hole mobility. The results are shown in Figure 4. (b) (c) and the values of E_g were found to be 3.05 eV, 2.25 eV for ZO and SZO. These results manipulate the SZO exhibit improved absorption ability in the visible range which suggests that the solarphotocatalytic

activity would be greatly increased by the effective absorption of visible light compared to ZO.

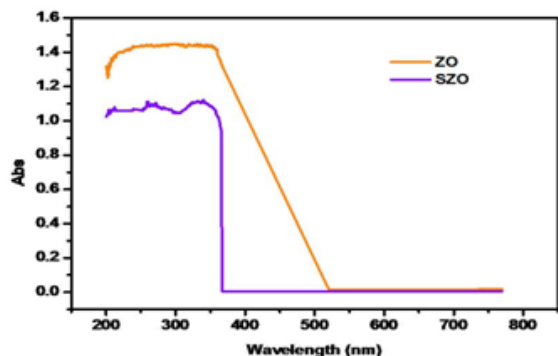


Figure 4 (a): UV-vis- DRS of ZO and SZO

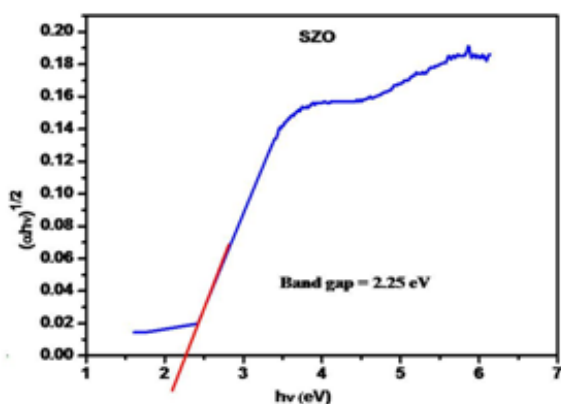
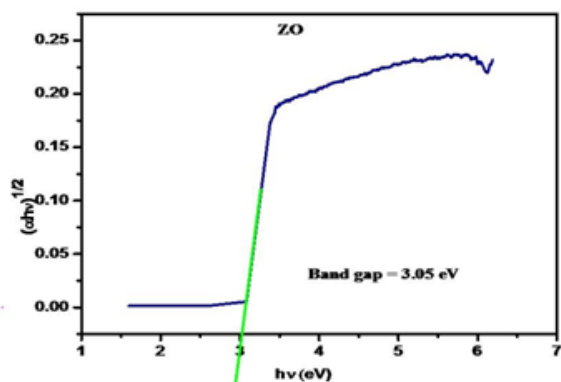


Figure 4(b): Tauc plot of ZO (c) Tauc plot of SZO

3.2 . FT-IR

FT-IR spectrums of SZO are shown in Figure 5. It has been reported that the peaks around 1020 and 674 cm^{-1} correspond to stretching vibration of ZnO [58]. The peaks 1588 cm^{-1} and 3442 cm^{-1} represent the diverse function groups of absorbed biomolecules on the surface of the ZnO nanoparticles [27]. The sharp peak at 1404 cm^{-1} corresponded to the C-N stretching mode of the aromatic amine group. The band at 1588 cm^{-1} can be assigned to the amide I band of the proteins and aromatic ring and 3442 cm^{-1} was related to N-H stretching [28, 29]. The position of peaks indicated presumably some secondary metabolites such as tannins, flavonoids, alkaloids and cartenoids which are abundant in the plant extract have interacted with ZnO surface making ZnO to be received visible light irradiation [30].

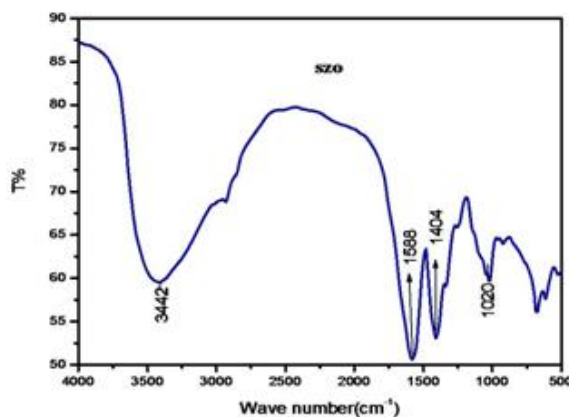


Figure 5: FTIR spectrum of SZO

3.3. XRD

The as-synthesized nanoparticle was examined for XRD pattern and was shown in Figure 6. XRD pattern is in good agreement with the standard peaks for the face centered cubic phase of ZnO (JCPDS card 65-2880), and the strong peaks (111) and (220) planes was observed with 2θ values of 32.97° and 59.01°. The average crystallites size was calculated using the Debye's scherrer equation [63].

$$D = \frac{k\lambda}{\beta \cos\theta} \quad (3.2)$$

where β is the full width at half height maximum of the most intense 2θ peaks, is the shape factor (0.89). θ , λ are incident angle and wavelength of X-rays respectively. The average crystal size of ZO decreases with the addition of plant extract [31] and the crystalline size of ZO and SZO are 23 nm and 17 nm respectively.

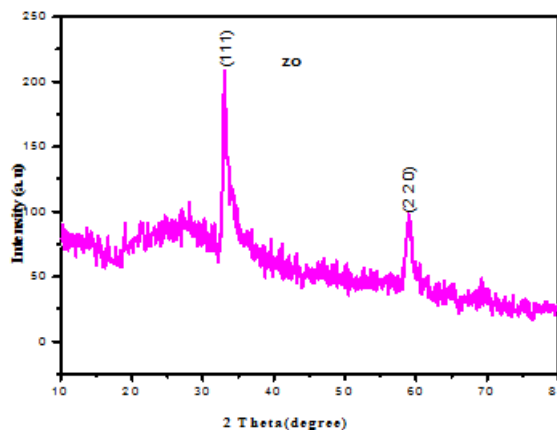


Figure 6(a): XRD image of ZO

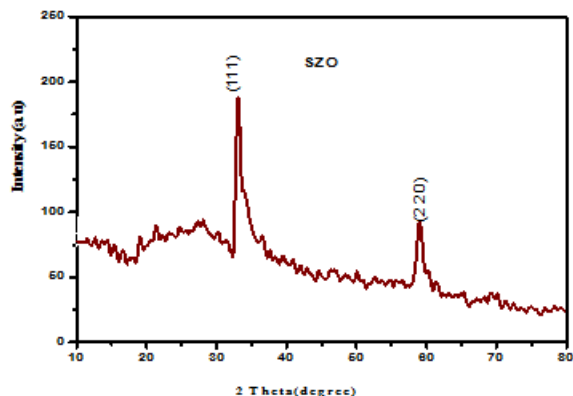


Figure 6(b): XRD image of SZO

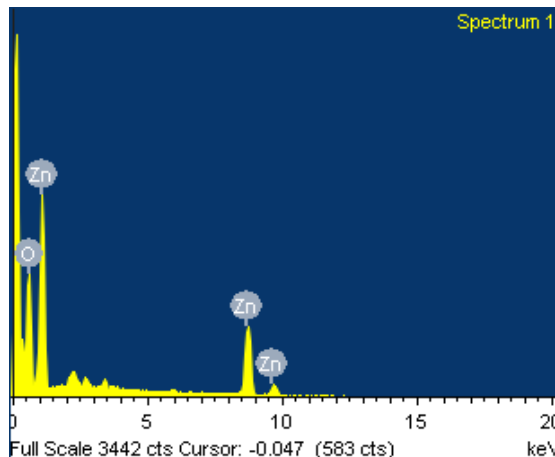


Figure 8(a): EDX spectrum of ZO

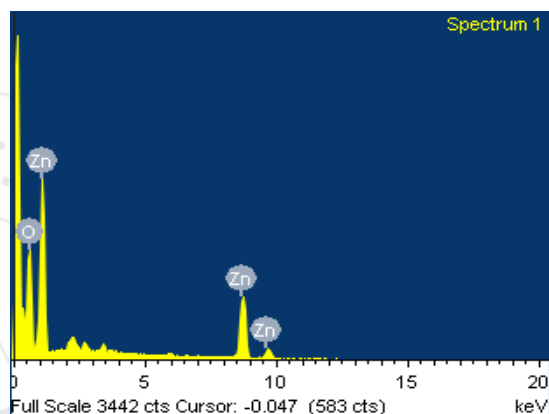


Figure 8(b): EDX spectrum of SZO

3.4. SEM and EDX

Figure 7(a) and (b) shows the SEM image of ZO and SZO respectively and is observed that the ZO sample is composed of small plates and needle structure disappeared and their surfaces are smooth with the addition of plant extract [32]. The antioxidant present in the plant extract acts as a surface modifier and Figure 8. shows the EDX spectrum of ZO and SZO. The highest intense peaks observed at 0.5 keV and 2.32 keV correspond to O and Zn element present in the ZO and SZO nanoparticles.

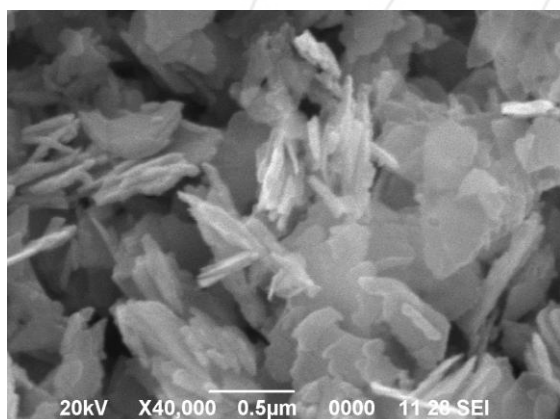


Figure 7(a): SEM image of ZO

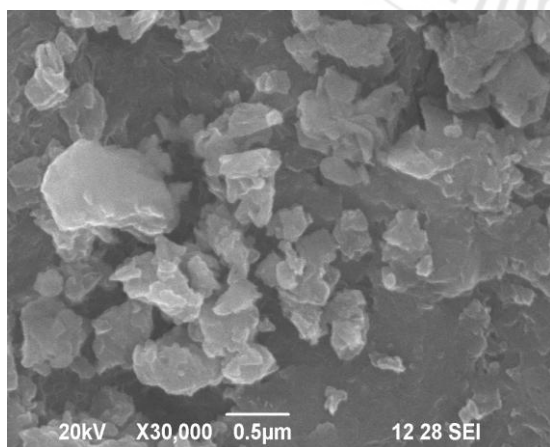


Figure 7(b): SEM image of SZO

Table 1: EDX elemental analysis of ZO and SZO

S. No	Sample	Atomic %	KeV
1	ZO	Zn= 24.43 O = 74.05	Zn = 1.01, 8.63, 9.57 keV O = 0.52 keV
2	SZO	Zn= 24.43 O = 74.05	Zn = 1.01, 8.63, 9.57 keV O = 0.52 keV

3.5. Solarphotocatalytic activity of SZO

Photocatalytic experiments was carried out with an initial FU concentration of 10μm with catalyst dosage of 0.10 g/L was shown in Figure9. Further more SZO (99%) source a enhanced photocatalytic activity when compare to ZO (80%).

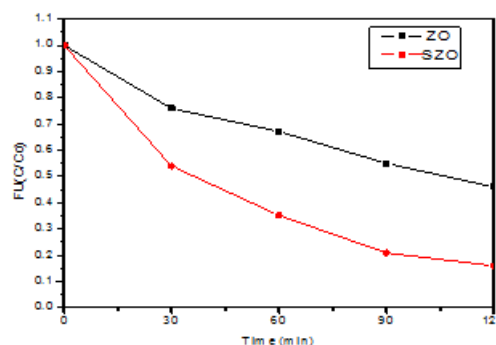


Figure 9: Effect of various catalyst on solarphotocatalysis of FU

3.5.2. Effect of catalyst concentration

The influence of the catalyst concentration of FU dye has been studied by using different dosages of SZO ranging from 0.050 - 0.150 g/L was shown in Figure 10. It has been found that the photodegradation percentage increase with increasing SZO dosage from 0.050 to 0.10g/L, thereafter, increase in photocatalyst loading (0.15 g/L) decrease the degradation. The observed enhancement in the photodegradation is probably due to an increased number of available sites on ZnO surface. Further increasing of SZO loading may cause the aggregation of free catalyst, increased opacity and a decrease in the penetration of light as a result of the increased scattering effect [33].

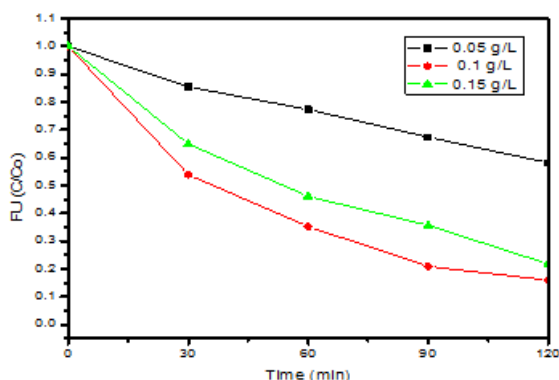


Figure 10: Effect of SZO dosage on the photodegradation of FU

3.5.3. Effect of initial dye concentration on the photodegradation of FU

After optimizing the photocatalyst dosage, the effect of initial dye concentration ranging from 5 to 10 μm on the photodegradation of FU was investigated [34]. The obtained results are shown in Figure 11. It has been observed that the photodegradation increased with increasing in dye concentration from 5 to 10 μm the photodegradation increase, this may be due to the fact that as the dye concentration was increased and more dye molecules were available for consecutive degradation.

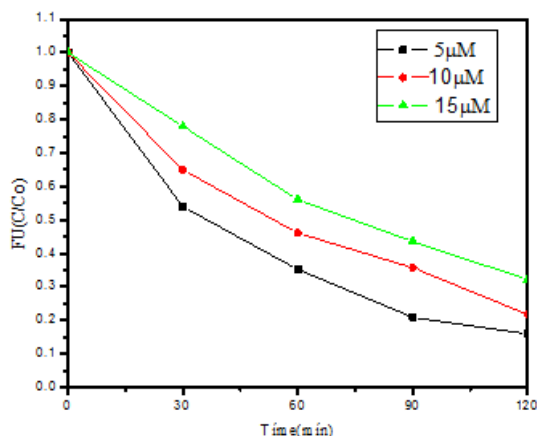


Figure 11: Effect of initial FU concentration on its photodegradation

3.5.4 Kinetic study FU

The solar photocatalytic reaction kinetics of FU degradation experiments follows pseudo first order equation and it can be expressed as follows [35]:

$$-\ln \frac{C}{C_0} = kt \quad (3)$$

where C_0 is the initial concentration of FU at $t=0$ min, is the concentration of FU at irradiation time 't' and k is the rate constant. The plot of $-\ln(C/C_0)$ versus irradiation time 't' is depicted in for the degradation of FU in the presence of ZO and SZO photocatalyst. Pseudo first order rate constants are evaluated from the slopes of $-\ln(C/C_0)$ versus time plot. The rate constant of SZO (1.69×10^{-2}) was higher than of ZO (7.17×10^{-2}) manifesting that addition of plant extract solanum xanthocarpum is apparently an effective method to improve the visible light induced photocatalytic efficiency are shown in Figure 12.

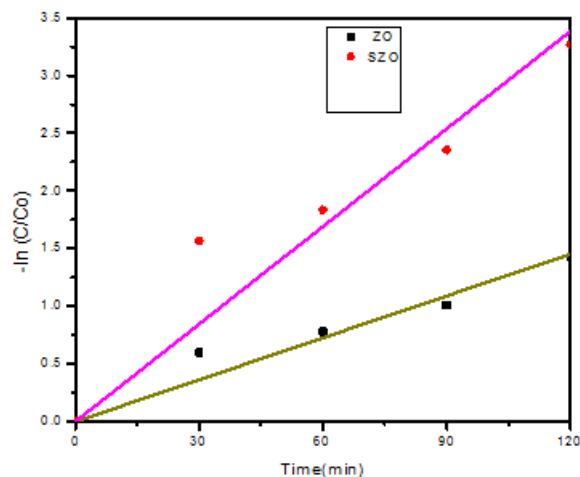


Figure 12: Kinetic plot of $-\ln(C/C_0)$ versus irradiation time for the photodegradation of FU

4. Conclusion

Solanum xanthocarpum plant was used to synthesize ZnO nanoparticles through green method. The structure, morphology and optical properties of the nanoparticles were confirmed by XRD, SEM, EDX, FT-IR, and UV-vis DRS measurements. The highest degradation efficiency was shown to be 99% degradation of FU in 120 min at a dye concentration of 10 μm with catalyst dosage of 0.10g/l. It follows pseudo first order kinetic with a rate constant of 1.69×10^{-2} for SZO was higher than of ZO (7.17×10^{-2}).

Acknowledgement

The authors want to acknowledge the Department of Chemistry Theni Kammavar Sangam College of Arts and Science, Theni, for providing necessary facilities for this project.

References

- [1] T.F. Robinson, G. McMullan, R. Marchant, P. Nigam, Remediation of dyes in textile effluent: a critical review on current treatment technologies with a proposed alternative," *Bioresource Technology*, vol. 77, no. 3, pp. 247-255, 2001.
- [2] P.P. Zamora, A. Kunz, S.G. Moraes, R. Pelegrini, P.C. Moleiro, J. Reyes, N. Duran, Degradation of reactive dyes I. A comparative study of ozonation, enzymatic and photochemical processes *Chemosphere* 38, pp 835- 852 (1999).
- [3] L. Ladakowicz, M. Solecka, R. Zylla, Biodegradation, decolorization and detoxification of textile wastewater enhanced by advanced oxidation processes, *Journal of Biotechnology* 89, pp 175 –185, (2001).
- [4] D. Georgiou, P. Melidis, A. Aivasidis, K. Gimouhopoulos, Degradation of azo-reactive dyes by ultraviolet radiation in the presence of hydrogen peroxide, *Dyes and Pigments* 52, pp 69-78, (2002).
- [5] J. Bao, M.A. Zimmler, F. Capasso, Broadband ZnO Single-Nanowire Light-Emitting Diode, *Nano Letters* 6, pp 1719-1722, (2006).
- [6] X.D. Bai P.X. Gao, Z.L. Wang, Dual-mode mechanical resonance of individual ZnO nanobelts, *Applied Physics Letters* 82, pp 4806-4810, (2003).
- [7] H.F.Lin, S.C. Liao, S.W. Hung, The dc thermal plasma synthesis of ZnO nanoparticles for visible-light photocatalyst, *Journal of photochemistry and Photobiology A*, 174, pp 82-87, (2005).
- [8] J.H. Sun, S.Y. Dong, Y. K. Wnag, S.P. Sun, Preparation and photocatalytic property of a novel dumbbell-shaped ZnO microcrystal photocatalyst, *Journal of Hazardous Materials* 172, pp 1520-1526, (2009).
- [9] K.J. Kim, P.B. Kreider, C. Choi, C.H. Chang, H.G. Ahn, Visible-light-sensitive Na-doped p-type flower-like ZnO photocatalysts synthesized via a continuous flow microreactor, *RSC Adv.* 3, pp 12702-120709, (2013).
- [10] K. Mor, H.E. Prakasam, O.K. Varghese, K. Shanker, C.A. Grimes, Vertically Oriented Ti-Fe-O Nanotube Array Films: Toward a Useful Material Architecture for Solar Spectrum Water Photoelectrolysis, *Nano Letters*, 7, pp 2356 – 2364, (2007).
- [11] X.F. Chen, X.C. Wang, Y.D. Hou, J.H. Huang, L. Wu, X.Z. Fu, The effect of postnitridation annealing on the surface property and photocatalytic performance of N-doped TiO₂ under visible light irradiation, *Journal of Catalysis* 255, pp 59-67 (2008).
- [12] S.Y. Kuang, L.X. Yang, S.L. Luo, Q.Y. Cai, Fabrication, characterization and photoelectrochemical properties of Fe₂O₃ modified TiO₂ nanotube arrays, *Applied Surface Science* 255, pp 7385-7388, (2009).
- [13] K. Vignesh, R. Priyanka, M. Rajarajan, A. Suganthi, Photoreduction of Cr(VI) in water using Bi₂O₃-ZrO₂ nanocomposite under visible light irradiation, *Material science science and Engineering B*, 178 pp 149-156, (2013).
- [14] C.W.E. van Eijk, Development of inorganic scintillators, *Nuclear Instruments and Methods in Physics Research Section A: Accelerators, Spectrometers, Detectors and Associated Equipment*, 392 (1997) pp 285-290.
- [15] M.A. Mahmood, S. Baruah, J. Dutta, Enhanced visible light photocatalysis by manganese doping or rapid crystallization with ZnO nanoparticles, *Materials Chemistry and Physics*, 130(1–2) pp 531-532 (2011).
- [16] Y. Liu, G. Li, R. Mi, C. Deng, P. Gao, An environment-benign method for the synthesis of p-NiO/n-ZnO heterostructure with excellent performance for gas sensing and photocatalysis, *Sensors and Actuators B: Chemical*, Volume 191, February 2014, Pages 537-544.
- [17] N.V. Kaneva, D.T. Dimitrov, C.D. Dushkin, Effect of nickel doping on the photocatalytic activity of ZnO thin films under UV and visible light, *Applied Surface Science*, 257, pp 8113-8120 (2011).
- [18] M.N. Khan, M.A. Hinai, A.A. Hinai, J. Dutta Visible light photocatalysis of mixed phase zinc stannate/zinc oxide nanostructures precipitated at room temperature in aqueous media *Ceramics International*, 40(6), 8743-8752, (2014).
- [19] D. Li, J.F. Huang, L.Y. Cao, J.Y. Li, H.B.O. Yang, C.Y. Yao, Microwave hydrothermal synthesis of Sr²⁺ doped ZnO crystallites with enhanced photocatalytic properties *Ceramics International*, 40(2), pp 2647-2653 (2014).
- [20] Y. Zong, Z. Li, X. Wang, J. Ma, Y. Men, Synthesis and high photocatalytic activity of Eu-doped ZnO nanoparticles *Ceramics International*, 40(7), pp10375-10382 (2014).
- [21] C. Yu, K. Yang, Q. Shu, J.C. Yu, F. Cao, X. Li, Preparation of WO₃/ZnO Composite Photocatalyst and Its Photocatalytic Performance *Chinese Journal of Catalysis*, 32(3–4), pp 555-565, (2011).
- [22] W.Y. Choi, A.termin, M.R. Hoffmann, The Role of Metal Ion Dopants in Quantum-Sized TiO₂: Correlation between Photoreactivity and Charge Carrier Recombination Dynamics, *Journal of physics and chemistry* 98(51), pp 13669-13679 (1994).
- [23] K. Fenga, W. Lib, S. Xieb, X. Lub, Nickel Hydroxide Decorated Hydrogenated Zinc Oxide Nanorod Arrays with Enhanced Photoelectrochemical Performance *Electrochimica Acta* 137, pp 108–113, (2014).
- [24] K. Vignesh, A.Suganthi, M.Rajarajan, S.A.Sara, Photocatalytic activity of AgI sensitized ZnO nanoparticles under visible light irradiation, *Powder Technology* 224, pp 331–337, (2012).
- [25] M.G. Nair, M. Nirmala, K. Rekha, A. Anukaliani, Structural, optical, photo catalytic and antibacterial activity of ZnO and Co doped ZnO nanoparticles, *Materials Letters* 65, pp 1797-1800, (2011).
- [26] G. Voicu, O. Oprea, B. S. Vasile, E. Andronescu, Photoluminescence and photocatalytic activity of Mn-doped ZnO nanoparticles, *Digest Journal of Nanomaterials and Biostructures* 8, pp 667-675, (2013).
- [27] F. Khaleghi, M.A. Khalilzadeh, J.B. Raof, M. Tajbakhsh, H.K. Maleh., Electrochemical oxidation of catechol in the presence of an aromatic amine in aqueous media, *J.Appl Electrochem* 39, pp 1651-1654, (2009).
- [28] M. Nasir, S. Bagwasi, Y. Jiao, F. Chen, B. Tian, J. Zhang, Characterization and activity of the Ce and N co-doped TiO₂ prepared through hydrothermal method, *Chemical Engineering Journal* 236, pp 388- 394, (2014).
- [29] B. Subash, B. Krishnakumar, V. Pandiyan, M. Swaminathan, M. Shanthi, An efficient nanostructured Ag₂S-ZnO for degradation of Acid Black 1 dye under

- day light illumination, Separation and Purification Technology, 96, pp 204-213, (2012).
- [30]B. Ahmmad, K. Leonard, M. Islam, J. Kurawaki, M. Muruganandhan, T. Ohkubo, Y. Kuroda, Green synthesis of mesoporous hematite (α -Fe₂O₃) nanoparticles and their photocatalytic activity, Advance powder technology, 24, pp 160-167, (2014).
- [31]S. Anandan, A. Vinu, N. Venkatachalam, B. Arabindoo, V. Murugesan, Photocatalytic activity of ZnO impregnated H β and mechanical mix of ZnO/H β in the degradation of monocrotophos in aqueous solution, Journal of Molecular Catalysis A: Chemical 256, pp 312-322, (2006).
- [32]J.Z. Kong, A.D. Li, X.Y. Li, H.F. Zhai, W.Q. Zhang, Y.P. Gong, H. Li, D. Wu, Photo-degradation of methylene blue using Ta-doped ZnO nanoparticle, Journal of Solid State Chemistry ,183, pp 1359-1367, (2010).
- a. Nageswara Rao, B. Sivasankar, V. Sadasivam, Kinetic studies on the photocatalytic degradation of Direct Yellow 12 in the presence of ZnO catalyst, Journal of Molecular Catalysis A: Chemical, 306, pp 77-81 (2009).
- [33]P. SathishKumar, R. Sivakumar, S. Anandan, J. Madhavan, P. Maruthamuthu, M. Ashokkumar, Photocatalytic degradation of Acid Red 88 using Au-TiO₂ nanoparticles in aqueous solutions, Water Research 42, pp 4878-4884 (2008).
- [34]W. Zhao, Z. Bai, A. Ren, B. Guo, C. Wu, Sunlight photocatalytic activity of CdS modified TiO₂ loaded on activated carbon fibers, Applied Surface Science 256, pp 3493-3498 (2010).

Author Profiles



Karthiga Rajendaran received the B.Sc in Madras University in 2003, M.Sc from Annamalai University in 2007, She completed her M.Phil in 2010 and Now, she is doing Ph.D research in Madurai Kamaraj University, India.



Sudha Annamalai received the B.Sc in Madurai Kamaraj University in 2015 and now she has completed her M.Sc in 2017 in the same University.